

# Theory of optical absorption by a localized carrier in an antiferromagnetic insulator

A. J. Millis and Boris I. Shraiman

*AT&T Bell Laboratories, Murray Hill, New Jersey 07974*

(Received 21 May 1992)

We calculate the optical absorption of a spin- $\frac{1}{2}$  carrier bound to a defect site in an insulating antiferromagnet. We show that when the defect potential is symmetric under interchange of the antiferromagnetic sublattices (as is believed to be the case in most doped high- $T_c$  parent compounds) the interaction of the carrier with the antiferromagnetic background leads to a low-frequency absorption feature near the zone-boundary magnon energy. This feature, however, is not consistent in peak position or total oscillator strength with the low-frequency absorption feature observed in lightly doped high- $T_c$  parent compounds. We suggest the observed feature is due to electron-phonon coupling.

## I. INTRODUCTION

High-temperature cuprate superconductors are produced by moderate (15–25%) doping of antiferromagnetic insulating “parent compounds” such as  $\text{La}_2\text{CuO}_4$ ,  $\text{Nd}_2\text{CuO}_4$ , and  $\text{YBa}_2\text{Cu}_3\text{O}_{6.0}$ . It is widely, although not universally, believed that proximity to the insulating phase and, in particular, interaction of dopant carriers with magnetic degrees of freedom is crucial to the physics of the high- $T_c$  materials.<sup>1</sup> For this reason there has been substantial experimental interest<sup>2–4</sup> in the properties of very lightly doped (1–5%) high- $T_c$  parent compounds, motivated in part by the hope of obtaining information about carrier-spin interactions by studying the evolution of material properties with doping at very low carrier concentration when one may expect that both carrier-carrier interactions and the effect of carriers on the magnetic order and excitation spectrum may be neglected. However, in order to add carriers to the high- $T_c$  “parent compounds” one must introduce dopant ions; in the limit in which these are very dilute, they produce potential fluctuations which localize the carriers. A theoretical estimate<sup>5</sup> suggests the binding energy  $E_B \sim 0.7$  eV. Thus, the study of a few carriers doped into a high- $T_c$  parent compound is necessarily the study of localized objects coupled to the magnetic excitation of an antiferromagnet.

Our work is motivated by the optical study by Cooper *et al.*<sup>3</sup> of  $\text{Nd}_2\text{CuO}_{4-x}$ ,  $\text{La}_2\text{CuO}_{4+x}$ , and  $\text{YBa}_2\text{Cu}_3\text{O}_{6+x}$ . They found a broad relatively strong absorption at  $\omega \sim 0.7$  eV, which was interpreted as the ionizing transition of a localized state with a binding energy  $E_B \sim 0.7$  eV, consistent with the previous theoretical calculation<sup>5</sup> and a relatively sharp but weak absorption feature near  $\omega = 0.2$  eV, which was interpreted as due to the excited states of the impurity broadened by interaction with other degrees of freedom in the crystal (such as spin waves).

In this paper we study theoretically the optical conductivity of a localized spin- $\frac{1}{2}$  carrier in an antiferromagnet. In Sec. II, we introduce the model Hamiltonian and distinguish the different regimes. In Sec. III, we analyze the model of a strongly localized carrier interacting with spin waves in some detail. In Sec. IV, we show that although

this model can explain the high-energy ( $\omega \sim 0.7$  eV) behavior, it does not provide a plausible explanation for the principal low-energy feature because it yields a much smaller oscillator strength, a higher peak frequency, and a less dramatic temperature dependence than is observed.<sup>6</sup> It is possible that the model may account for a secondary low-energy feature observed in some samples. In Sec. IV, we also discuss the alternative case of a carrier only weakly bound to an impurity and show that this interpretation also does not provide a satisfactory description of the optical data. Section V is a conclusion and discussion of alternative possible explanations.

## II. MODEL

### A. Qualitative considerations

We consider a bipartite lattice of sites. On each site but one there is an  $S = \frac{1}{2}$  local moment. On the remaining site there is a mobile carrier but no local moment. The amplitude for the carrier to hop from site to site is  $t$ ; the local moments are coupled via an antiferromagnetic Heisenberg exchange  $J \ll t$ . In addition we assume a local potential  $V$  which lowers the energy of a few sites relative to the others, and we assume that  $V$  is symmetric under the operation of interchanging the two sublattices of the bipartite lattice.

In the lightly doped high- $T_c$  parent compounds the lattice consists of the Cu sites of one of the  $\text{CuO}_2$  planes. The mobile carrier is either an electron residing predominantly on a Cu site, as in the case of the “electron-doped” system  $\text{Nd}_2\text{CuO}_{4-y}$ , or a hole residing predominantly on planar oxygen sites, as in the case of hole-doped materials such as  $\text{La}_{2-x}\text{Sr}_x\text{CuO}_4$  or  $\text{YBa}_2\text{Cu}_3\text{O}_{6+y}$ . In the  $\text{Nd}_2\text{CuO}_{4-y}$  material (on which we focus in this paper), the dopant electron is provided by an out-of-plane oxygen vacancy which, because it sits underneath the center of a planar Cu—Cu bond, has the symmetry under sublattice interchange assumed above. (In  $\text{YBa}_2\text{Cu}_3\text{O}_{6+x}$  and  $\text{La}_{2-x}\text{Si}_x\text{CuO}_4$  the impurity potential also has the sublattice symmetry.<sup>5</sup>)

The parameter values  $t \approx 0.5$  eV for the carrier hopping and  $J \approx 0.1$  eV for the magnetic exchange are by

now well established<sup>7,8</sup> for the  $\text{CuO}_2$  materials. The strength of the impurity potential is not as clear. A naive estimate,  $V_{\text{Coul}} = e^2/\epsilon r$ , using the measured high-frequency dielectric constant  $\epsilon \approx 5$  and setting  $r$  equal to the distance between the impurity and the  $\text{CuO}_2$  plane yields a very high value  $\sim 5$  eV. A theoretical calculation<sup>5</sup> found a binding energy  $E_B$  of order 0.5–1.0 eV, and a small bound-state radius of order 1–2 lattice constants. This conclusion depends strongly on the dielectric constant used. However, optical measurements on nominally pure samples reveal a very large low-frequency dielectric constant: for uniform ( $q=0$ ) electric fields parallel to the  $\text{CuO}_2$  plane at  $\omega$  less than the phonon frequency values  $\epsilon \sim 30$  have been reported,<sup>9</sup> these large values of  $\epsilon$  suggest that the high- $T_c$  materials are very polarizable at low frequencies. In the  $\text{CuO}_2$  planes the oxygen is supposed to have a substantial amplitude to be in the highly polarizable  $\text{O}^{2-}$  configuration. The large polarizability could lead to a strong screening of the impurity potential and thus to a dramatic reduction in the binding energy. However, computation of the binding energy requires knowledge of the static ( $\omega=0$ ) dielectric function on length scales comparable to the size of a unit cell for electric fields with a substantial out-of-plane component. To our knowledge this has not been reliably calculated or measured. Unfortunately, experimental evidence for or against the strong binding case is also ambiguous. On the one hand, optical absorption measurements on lightly doped cuprates,<sup>6</sup> reproduced in Fig. 1, reveal a strong feature at  $\omega \approx 0.7$  eV which has been interpreted<sup>6</sup> as the unbinding of the bound state with the binding energy consistent with theoretical predictions. On the other hand, transport measurements<sup>2,4</sup> on lightly doped samples indicate a rapid temperature dependence of the conductivity combined with a reasonably large room-temperature value. Analysis of these in terms of a variable range hopping model<sup>4</sup> suggests a rather low binding

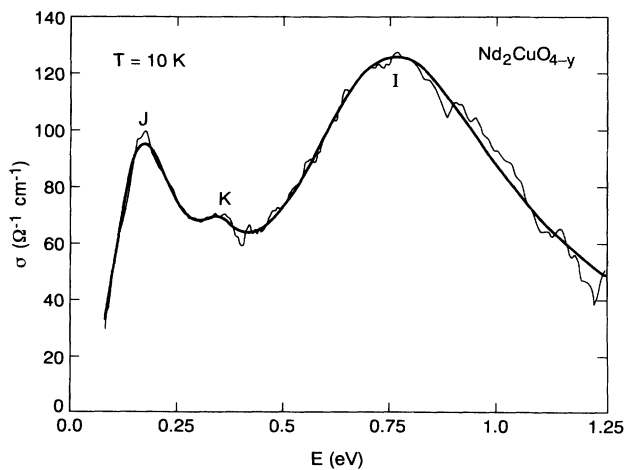


FIG. 1. Optical absorption vs energy for lightly doped insulating  $\text{Nd}_2\text{CuO}_{4-y}$  with  $y \sim 0.035$ , from Ref. 6. The feature  $E_I$  has been interpreted as arising from the ionization of a defect state, while the feature  $E_J$  and the weak feature which may exist at  $E_K$  may be due to excitation of internal degrees of freedom of the defect.

energy  $E_B < 0.1$  eV. The latter conclusion may not be definitive for two reasons. One is that the dopant density in the samples studied is high enough that impurity banding effects may be important. In this case the apparent binding energy would be the property of the impurity band and would not simply be related to the binding energy of an ion on an isolated impurity. Another more subtle possibility involves a “Franck-Condon” effect which could lead to drastically different low- and high-frequency responses, (i.e., thermally activated hopping conductivity and optical conductivity, respectively) due to the coupling to a highly polarizable lattice.<sup>10</sup>

In any event, it seems to us that the situation is sufficiently unclear that a further examination of the experimental consequences of both the weakly bound and the strongly bound models is warranted. We therefore discuss the optical conductivity due to a single carrier which may be weakly ( $E_B \ll t$ ) or strongly ( $E_B \gtrsim t$ ) bound to an impurity site, and compare the results to the data. In the weak binding case the impurity potential is almost irrelevant, and we may determine the optical conductivity by suitable modification of known results for the  $t$ - $J$  model. In the strong binding case, a more detailed calculation is required. We will show that in the strong binding case there are interesting lower-energy features associated with carrier-spin interactions in addition to the absorption feature occurring at a frequency comparable to the binding energy  $E_B$ . Proper treatment of these in the strong binding limit requires a model Hamiltonian which we derive in Sec. II B.

### B. Model Hamiltonian for the strong binding case

We now consider the strong binding symmetric case in more detail. It is useful to consider first the simplifying limit where the impurity potential is so strong that the localized carrier is confined to two sites (see Fig. 2). In this simple model the impurity is described by four states, which we may label by the site on which the carrier sits and the spin of the local moment on the other site. The four states of the impurity are mixed by the hopping matrix element,  $t$ , which moves the hole from one site to the other, and by the exchange coupling  $J$  which connects

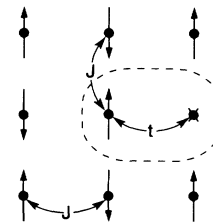


FIG. 2. Model for strongly bound carrier interacting with spins. The carrier is assumed bound by an impurity potential (not shown) to the two sites circled with the dotted line. The carrier may hop from one site to the other via a matrix element,  $t$ . On the site not occupied by the carrier resides a spin. This spin couples to the three nearest-neighbor spins of the antiferromagnet via a Heisenberg coupling,  $J$ .

the impurity spin to the neighboring spins in the lattice. In the high- $T_c$  systems  $t$  ( $\sim 0.5$  eV)  $>$   $J$  ( $\sim 0.12$  eV). In the limit  $J=0$ , the  $t$  term splits the states into two doubly degenerate (because of spin) pairs: bonding, even under sublattice interchange, and antibonding, odd under sublattice interchange. Bonding and antibonding states are split by an energy of order  $t$ . Discussion of the magnetic effects occurring for nonzero  $J$  requires a model for the magnetic properties of the background lattice. We assume two sublattice Néel antiferromagnetic order, with the ordered moment  $\mu$  oriented in the  $\pm z$  direction and assume that the excitations are described by linear-spin-wave theory. The coupling to the static moments of the Néel order distorts the wave functions, so that, e.g., in what was previously the spatially symmetric bonding spin-up state, the spin acquires an extra amplitude (of order  $J/t$ ) to be on the up sublattice, etc. The twofold degeneracy of the ground state is preserved because the Néel state is invariant under the combination of sublattice interchange and time reversal which flips all spins. However, the impurity degrees of freedom are also coupled to the spin-wave excitations; this leads to a nontrivial interacting problem.

The effective Hamiltonian corresponding to the strong impurity binding limit depicted in Fig. 2 is derived in Ap-

pendix A, and appears in Eq. (2.1). It is clear on physical grounds that in the more general situation of binding energy large compared to  $J$  but not necessarily large compared to  $t$ , one must obtain a very similar Hamiltonian, with a ground state which is (in the absence of magnetic coupling) symmetric under sublattice interchange, one or more excited states (which may, in fact, be delocalized) including at least one which is odd under sublattice interchange (in the absence of magnetic coupling), and therefore is optically active. The form of the coupling to the spin-wave excitations is determined by symmetry and thus will be the same as that found in the simplified model but with coefficients which may differ by numerical factors. In Eq. (2.1)  $c_{b\sigma}^\dagger$  ( $c_{a\sigma}^\dagger$ ) creates a bonding (antibonding) state of spin  $\sigma$ ,  $\alpha_k^\dagger$  and  $\beta_k^\dagger$  are the usual Holstein-Primakoff spin-wave operators creating magnons of energy  $\omega_k$ , and  $M_k$  and  $N_k$  are the form factors. In the long-wavelength limit  $M_k \sim \sqrt{\omega_k}$  and  $N_k \sim 1/\sqrt{\omega_k}$ , and the terms involving  $M_k$  and  $N_k$  correspond to fluctuations of the uniform and staggered magnetization, respectively. The energy  $\Delta$  gives the splitting between bonding and antibonding states and is of order  $t$ .  $g_1$ ,  $g_2$ , and  $g_3$  are coupling constants with  $g_1$  and  $g_3$  of order  $J$  and  $g_2$  of order  $J^2/t$ . Precise values of the various parameters in the limit of strong binding are derived in Appendix A. We have

$$H = \frac{1}{2}\Delta \sum_{\sigma} (c_{a\sigma}^\dagger c_{a\sigma} - c_{b\sigma}^\dagger c_{b\sigma}) + g_1 \left[ (c_{b\uparrow}^\dagger c_{b\downarrow} + c_{a\uparrow}^\dagger c_{a\downarrow}) \sum_k (M_k \alpha_k^\dagger + M_k^* \beta_k) + \text{H.c.} \right] \\ + g_2 \left[ (c_{a\uparrow}^\dagger c_{b\downarrow} - c_{b\uparrow}^\dagger c_{a\downarrow}) \sum_k (M_k \alpha_k^\dagger + M_k^* \beta_k) + \text{H.c.} \right] + g_3 \left[ (c_{a\uparrow}^\dagger c_{b\downarrow} + c_{b\downarrow}^\dagger c_{a\uparrow}) \sum_k (N_k \alpha_k^\dagger - N_k^* \beta_k) + \text{H.c.} \right]. \quad (2.1)$$

We represent the applied electric field by a vector potential,  $A \equiv \hat{\mu} \cdot \mathbf{A}_\mu$  defined as the component of the electromagnetic vector potential along the bond direction  $\hat{\mu}$  of the localized impurity state. The coupling  $H_A$  of the carrier to the field may be derived similarly and is

$$H_A = iefA \sum_{\sigma} (c_{a\sigma}^\dagger c_{b\sigma} - c_{b\sigma}^\dagger c_{a\sigma}). \quad (2.2)$$

The optical coupling constant  $f$  is of order the hopping  $t$  and  $e$  is the electric charge.

The Hamiltonian, Eq. (2.1), describes an electron which may be in one of two orbital states ( $b$  or  $a$ ) and one of two spin states (up or down), interacting with magnons. There are two types of electron-magnon interactions: the “ $g_1$ ” processes in which the spin is flipped but the orbital state is not changed, and the  $g_{2,3}$  processes, in which both the spin and the orbital state are changed. Because exciting the electron from a  $b$  to an  $a$  state involves an energy cost of order  $t \gg g_{2,3}$ , it is reasonable when studying low-energy properties to neglect the  $g_{2,3}$  processes. The effects of  $g_{2,3}$  are considered in Sec. III and Appendix B. The  $g_1$  term leads to a “localized-spin-polaron” effects in which the presence of the localized spin leads to a distortion of the Néel order while the coupling to spin excitations means that the local spin is not an eigenstate of  $\sigma_z$ . Determining the effects of the  $g_1$  term is difficult because the formal perturbation expansion in  $g_1$  is really an expansion in  $(g_1 \sum_k \omega_k^{-1})$  which is of

order 1 because the only dimensionful parameter in the low-energy theory is  $J$ . We hope to give a detailed account of the low-energy spin dynamics elsewhere. For the optical conductivity the relevant quantity is the Green's function  $G_{b\sigma}(t) = \langle T \{ c_{b\sigma}^\dagger(t) c_{b\sigma}(0) \} \rangle$ , which is essentially the probability of finding the electron in spin state  $\sigma$  at time  $t$  if it was known to be in spin state  $\sigma$  at time 0. For  $g_1=0$  the probability is 1, which means that the spectral function  $A(\omega) = \text{Im}G(\omega)$  [where  $G(\omega) = \int dt e^{i\omega t} G(t)$ ] takes the simple form  $A(\omega) = \delta(\omega)$ . We analyze the effect of a nonzero  $g_1$  via the “noncrossing approximation,” which amounts to summing the diagrams shown in Fig. 3 and which we believe gives qualitatively correct results if the effective interaction is not too large. Within this approximation the interaction correction to the spectral function electron-magnon interactions may be parametrized by the quantity  $\lambda = g_1^2 \sum_k |M_k|^2 / \omega_k^2$ . By summing the diagrams shown in Fig. 3 we find, as one would expect, at  $T=0$  the strength of the  $\delta$  function is reduced to  $1/(1+\lambda/2\pi)$  and the weight is redistributed to higher frequencies. The existence of a  $\delta$ -function peak<sup>11</sup> in  $A(\omega)$  will be important for our calculation of the optical conductivity. For  $T>0$  we find the  $\delta$  function is broadened, in such a way that, for  $\omega^*(t) < \omega < T$ ,

$$A(\omega, T) \cong \frac{\lambda/2}{(1+\lambda/2\pi)^2} \frac{T}{\omega},$$

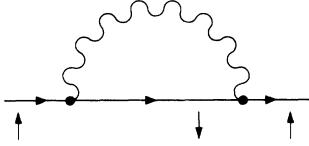


FIG. 3. Feynman diagram for the impurity self-energy. The wiggly line denotes a magnon, the solid line the impurity propagator, and the dot denotes the vertex  $g_1 M_k$ . The arrow denotes the direction of the impurity spin.

and for  $\omega < \omega^*(T)$ ,

$$A(\omega, T) = \frac{\lambda/2}{(1 + \lambda/2\pi)^2} \frac{T}{\omega^*(T)},$$

with the cutoff  $\omega^*(T)$  such that

$$\lim_{T \rightarrow 0} \int_0^T A(\omega, T) = \frac{1}{1 + \lambda/2\pi}.$$

Typical results for  $A(\omega)$  within this approximation are shown in Fig. 4.

### III. OPTICAL CONDUCTIVITY: STRONGLY BOUND LIMIT

We may compute the conductivity by applying the standard linear response theory to the Hamiltonian (2.1). It is clear that the largest contribution to the calculated conductivity comes from processes in which the electron is transferred from a  $b$  state to an  $a$  state. The precise functional form of this contribution cannot be reliably calculated at this point since it requires detailed information about the “ $a$ ” states. It is, however, useful to estimate the total optical spectral weight,  $\omega_p^2$ , which is defined in terms of the real part,  $\sigma_1$ , of the optical conductivity, as

$$\omega_p^2 = 8 \int_0^\infty \sigma_1(\omega) d\omega. \quad (3.1)$$

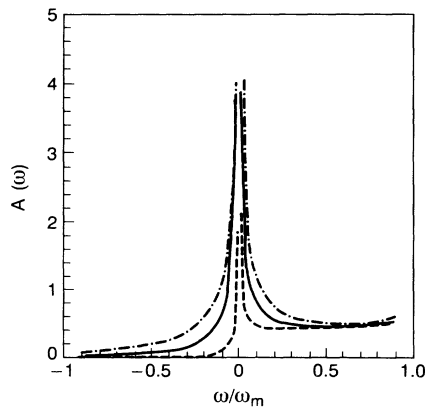


FIG. 4. Impurity spectral function calculated from the diagram shown in Fig. 3, for several temperatures,  $T$ , for coupling constant  $\lambda=1.0$ . The behavior at zero temperature is a  $\delta$  function at  $\omega=0$  followed by an essentially  $\omega$ -independent background. For  $T > 0$  the behavior for  $\omega \lesssim T$  is  $\sim T/\omega$ , cut off at a very low frequency (not shown) in such a way that the total area is  $T$  independent.

One may derive an expression for  $\omega_p^2$  by using arguments very similar to the standard derivation of the  $f$ -sum rule: one finds an operator  $Q$  such that the commutator of  $Q$  and the Hamiltonian  $H$  reproduces the current operator given by the coefficient of  $A$  in Eq. (2.2). In the present case

$$Q = \frac{ef}{\Delta} \sum_{\sigma} (c_{a\sigma}^{\dagger} c_{b\sigma} + c_{b\sigma}^{\dagger} c_{a\sigma}) + O\left[\frac{g}{\Delta}\right]. \quad (3.2)$$

It is then a matter of simple algebra to show that

$$\begin{aligned} \frac{\omega_p^2}{8} &= \left\langle \left[ [Q, H], Q \right] \right\rangle \\ &= \frac{f^2 e^2}{\Delta} \sum_{\sigma} \langle (c_{b\sigma}^{\dagger} c_{b\sigma} - c_{a\sigma}^{\dagger} c_{a\sigma}) \rangle + O\left[\frac{gf}{\Delta}\right]. \end{aligned} \quad (3.3)$$

It is clear that the expectation value is  $[1 - O(g^2/\Delta^2)]$ , and thus the total spectral weight is of order  $t$ . It is also clear that although most of the total spectral weight will occur at frequencies of order  $\Delta$ , some spectral weight will exist at lower frequencies because the terms proportional to  $g_2$  and  $g_3$  in the Hamiltonian, Eq. (2.1), mean that processes are possible in which the particle is excited from the  $b$  to  $a$  state and then goes back to the  $b$  state of opposite spin by emitting a magnon. Because the coupling constants  $g_2$  and  $g_3$  are of order  $J$  and the process involves a virtual state with an energy of order  $\Delta$ , it is reasonable to study these processes via perturbation theory in  $g_{2,3}/\Delta$ . The most efficient way to implement this perturbation theory is via a canonical transformation which perturbatively eliminates the terms mixing the  $a$  and  $b$  states in Eq. (2.1). The details of the perturbation theory are given in Appendix B; the resulting Hamiltonian,  $H'_1$ , restricted to the manifold of “bonding” states, may be written, to leading order in  $g_{2,3}/\Delta$ ,

$$\begin{aligned} H'_1 &= g_1 \left[ c_{b\uparrow}^{\dagger} c_{b\downarrow} \sum_k (M_k \alpha_k + M_k^* \beta_k^{\dagger}) + \text{H.c.} \right] \\ &+ \sum_k \omega_k (\alpha_k^{\dagger} \alpha_k + \beta_k^{\dagger} \beta_k). \end{aligned} \quad (3.4)$$

The coupling of the electric field to the low-energy manifold is

$$H'_A = efA \sum_k \hat{J}_k \quad (3.5a)$$

with the effective current operator  $\hat{J}_k$  given by

$$\hat{J}_k = Q_k (\alpha_k^{\dagger} + \beta_k) c_{b\uparrow}^{\dagger} c_{b\downarrow} - \text{H.c.} \quad (3.5b)$$

and

$$Q_k = \left[ \frac{g_2 M_k}{\Delta} + \frac{g_3 \omega_k N_k^*}{\Delta^2} \right]. \quad (3.5c)$$

The effective Hamiltonian shows that the process in which an electron in the  $b$  orbital flips its spin and emits a magnon is optically allowed, although the matrix element is rather small, of order  $(J/t)^2$ , because  $g_2 \sim J^2/t$  while both  $g_3$  and  $\omega_k \sim J$ . We have verified that  $g_3$ , i.e., the coupling to the staggered magnetization, occurs only in the combination  $g_3 \omega_k$  also in the next order of perturba-

tion theory. We suspect that this is general, i.e., that the effective Hamiltonian for low-energy optical absorption has an expansion in powers of  $(J/t)^2$ . In the rest of this paper we consider only the leading-order Hamiltonians (3.4) and (3.5).

The optical conductivity can be calculated from the Kubo formula. The real part of the conductivity  $\sigma_1(\omega)$  is given by

$$\sigma_1(\omega) = \frac{e^2 f^2}{\omega} \text{Im} \int_0^\infty dt e^{i\omega t} \left\langle \left[ \sum_{k'} J_k(t), \sum_{k'} J_{k'}(0) \right] \right\rangle. \quad (3.6)$$

Because the Hamiltonian, (3.4) cannot be solved exactly one must compute  $\sigma_1$  by a formal perturbation expansion in  $g_1$ , as we did for the spectral function in Sec. II. We believe that the leading-order diagram, shown in Fig. 5(a) gives a qualitatively correct result. We have shown that one particular set of corrections [shown in Fig. 5(b)] may be summed to infinite order in  $g_1$  without changing the results in any essential way, and that other diagrams [such as those in Fig. 5(c)] vanish in low orders in perturbation theory.

The diagram shown in Fig. 5(a) may be easily evaluated. At  $T=0$ , it gives

$$\sigma_1(\omega) = \frac{e^2 f^2}{\omega} \sum_k |Q_k|^2 \delta(\omega - \omega_k). \quad (3.7)$$

The result, Eq. (3.7), is clearly proportional to  $\rho(\omega) = \sum_k \delta(\omega - \omega_k)$ , the magnon density of states at frequency  $\omega$ . Note that as  $\omega \rightarrow 0$  both  $Q_k$  and  $\rho(\omega)$  vanish as  $\omega$ , leading to  $\sigma_1(\omega) \sim \omega^2$  as  $\omega \rightarrow 0$ . Note also that as  $\omega$  approaches the magnon zone boundary  $\omega_m$ , the magnon density of states diverges as

$$\rho(\omega) \sim [(\omega - \omega_m)^{1/2} \ln(\omega_m - \omega)]^{-1}.$$

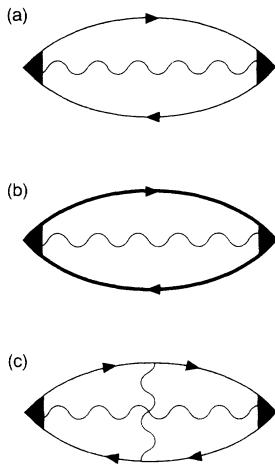


FIG. 5. Feynman diagrams used in the calculation of optical absorbtivity. The wiggly lines denote magnons, the triangular vertex is the optical matrix element of Eq. (3.5), and thin and thick solid lines denote impurity propagators with and without the self-energy calculated from the diagram in Fig. 3. The vertex corrections shown in (c) vanish.

Thus Eq. (3.7) predicts very small absorption at low frequencies and a divergence at  $\omega = \omega_m$ . Expression (3.7) for  $\sigma(\omega)$  is essentially the Fermi Golden Rule for the  $H'_A$  [Eq. (3.5a)] process, and thus corresponds to the joint density of states of the impurity and the emitted magnon.

The  $g_1$  processes do not regularize the divergence of  $\sigma(\omega)$  at  $\omega = \omega_m$ . However, the perturbative derivation of the effective Hamiltonian [(3.4) and (3.5a)] requires  $\Delta^{-1} g_3^2 \rho(\omega) \ll 1$ , which is violated for  $|(\omega - \omega_m)/\omega_m| < (J/t)^2$ , when the self-energy correction for the excited impurity state,  $a$ , cannot be neglected. Thus, we expect the divergence to be cutoff on that scale and the magnitude of  $\sigma_1$  to saturate at the value of order  $J/t$ . Note that the integrated low-energy spectral weight is  $\int_0^{\omega_L} d\omega \sigma_1(\omega) \sim O(J^3/t^2)$  ( $\omega_L \approx \omega_m$ ) and that the weight is concentrated near the  $\omega \approx \omega_m$  feature.

We now consider the temperature dependence of  $\sigma(\omega)$  within the framework of the effective Hamiltonian. The conductivity will have temperature dependence because, as discussed in the previous section, the impurity spectral function has temperature dependence. In particular, for  $T > 0$ , the impurity is no longer in a definite spin state, so the  $\delta$ -function contribution to the impurity spectral function is broadened, and the divergence  $\sigma$  due to the zone-boundary magnon emission is washed out at  $T > 0$  by  $g_1$  processes. We have studied this effect quantitatively by calculating the diagrams in Figs. 5(a) and 5(b) at finite temperature. We find that the  $T$  dependence of the optical absorption is very weak except near the peak at  $\omega = \omega_m$ ; in the range  $(\omega - \omega_m) < T$ , the conductivity varies at  $T^{-1/2}$ ; again for  $T/\omega_m < (J/\Delta)^4$  we expect this temperature dependence to saturate.

Thus, to summarize, we have argued that the carrier-spin mechanism leads to low-frequency absorption spread over a frequency scale  $\omega_L$  of order several times  $\omega_m$ ; the total spectral weight  $\int_0^{\omega_L} d\omega \sigma(\omega) \sim J^3/t^2$  and there is a pronounced,  $T$ -dependent peak at  $\omega_m$ . Results of calculations at different temperatures are shown in Fig. 6.

#### IV. COMPARISON WITH EXPERIMENT AND DISCUSSION

Let us now compare the expected behavior of  $\sigma(\omega)$  for a tightly localized carrier coupled to antiferromagnetic

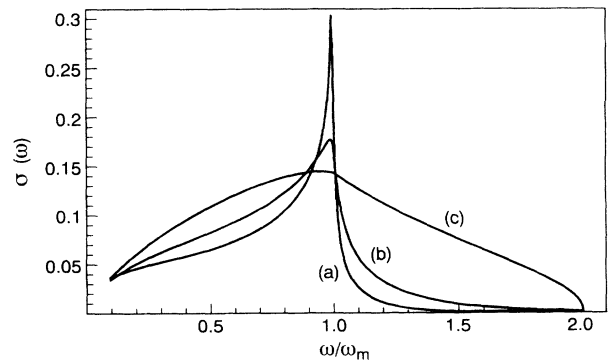


FIG. 6. Low-frequency optical conductivity calculated as described in the text for  $\lambda \approx 0.4$  and  $T/\omega_m = \frac{1}{16}$  (a),  $\frac{1}{8}$  (b), 1 (c).

(AFM) spin waves to the existing optical data<sup>6</sup> on weakly doped AFM insulators. The results of the previous section can be summarized by stating that the localized impurity absorption spectrum consists of (1) a broad feature at  $\omega \approx O(t)$ , with total spectra weight  $O(t)$ , corresponding to (damped) resonant transitions from the ground state to the optically active excited states, (2) a low-energy absorption peak at  $\omega \approx \omega_m$ , which is strongly asymmetric and carries  $O(J^3/t^3)$  fraction of the total spectral weight. The latter feature corresponds to the AFM zone-boundary magnon emission. While it is tempting to identify it with the observed main low-energy peak “J” shown in Fig. 1, the zone-boundary magnon energy is known from the neutron-scattering experiments<sup>12</sup> to be at  $\omega_m \approx 0.32$  eV, which is too high to be consistent with the feature J at  $\sim 0.2$  eV. Furthermore, the spectral weight of the observed “J” feature is significantly larger than predicted for the one-magnon process. The low-energy absorption feature we have calculated is more consistent with the weak absorption feature “K” observed at low  $T$  in some samples.

The failure of our simple model to explain the low-energy absorption peak “J” requires that the alternatives be considered. In particular, one may inquire into the relevance of the tightly bound carrier limit. Let us first consider the effect of a somewhat weaker impurity potential  $E_B \sim O(t)$ . In that case the carrier wave function will extend to many nearby sites forming, because of the background AFM correlation, a Brinkman-Rice “string” state.<sup>13</sup> The internal excitations of the string are on the scale  $J^{2/3}t^{1/3}$ , which is lower than the naive  $O(t)$  bonding-antibonding splitting for the tightly localized state. Thus, the resonant absorption for the carrier weakly localized in a string state would shift to a somewhat lower-energy scale compared with the strong localization case. On the other hand, the coupling of the carrier states to spin excitations, being governed by the same symmetry considerations (i.e., invariance under time reversal and sublattice interchange), remains essentially the same [i.e., governed by  $H_{\text{eff}}$  similar to that of Eq. (2.1)]; hence, so are our conclusions about the low-energy part of  $\sigma(\omega)$ .

Let us now discuss the weak binding limit where the binding energy  $E_B \ll J$  as proposed by Preyer *et al.*<sup>4</sup> In this impurity binding effects weak perturbation to the absorption to be that of a delocalized carrier, at least for  $\omega > E_B$ . The band structure of a carrier in an AFM has been intensively studied<sup>14,15</sup> and is known to consist of disjoint anisotropic valleys near the  $k = (\pm\pi/2, \pm\pi/2)$  points in the Brillouin zone with bandwidth of  $O(J)$ . The optical conductivity has been studied by many authors.<sup>15,16</sup> The quasiparticle<sup>15</sup> spectral weight is  $O(J/t)$ , leading to the corresponding Drude term in  $\sigma(\omega)$  with the spectral weight  $O(J)$  per carrier<sup>15</sup> corresponding to the  $O(t/J)$  quasiparticle mass enhancement. Since the total spectral weight is of  $O(t)$ , most of it is accounted for by the transitions to the excited “string” states represented by the incoherent part of the carrier spectral function. For  $\omega > J^{2/3}t^{1/3}$ ,  $\sigma(\omega)$  should be reasonably well described by the Brinkman-Rice approximation predicting<sup>16</sup>  $\sigma(\omega) \sim t\omega^{-1}$  (for large  $\omega$ ). One also expects a

feature at  $\omega \approx J^{2/3}t^{1/3}$  corresponding to the lowest optically active “string” excited state. Now it seems reasonable to assume that for  $\omega > J > E_B$  the impurity potential only weakly perturbs the results. Thus, for  $\omega > 0.2$  eV we would expect a conductivity which monotonically decreases with increasing  $\omega$ . In fact, as can be seen in Fig. 1, the observed conductivity *increases* with increasing  $\omega$  for  $0.2 < \omega < 0.7$  eV. For this reason we do not believe the weakly bound impurity model can account for the data.

## V. CONCLUSION

We have presented a theoretical study of the optical absorption spectrum of a carrier bound to a defect potential in an insulating antiferromagnet. We concentrated on the case of a carrier strongly bound ( $E_b \gg J$ ) by a potential which is symmetric under the interchange of the two sublattices of the antiferromagnetic. We showed that in this case the process in which the localized carrier flips its spin and emits a magnon is optically allowed and gives rise to low-frequency optical absorption strongly peaked at the zone boundary peaked at the zone-boundary magnon energy,  $\omega_m$ . We estimated the magnitude, functional form, and temperature dependence of this absorption. However, we found that the peak position, temperature dependence, and spectral weight of the theoretically predicted feature were not consistent with the low-energy feature observed in optical experiments on very lightly doped high- $T_c$  materials. We also argued that the alternative model of a weakly bound carrier ( $E_b < J$ ) led to a high-frequency ( $\omega > J$ ) conductivity very similar to that of one hole in a defect-free antiferromagnet. Known results from this problem are also inconsistent with the optical data.

A radically different possibility is that the peak at  $E_J$  is due to the electron-phonon interaction. Because the stoichiometric insulating cuprates are ionic crystals, one may expect the electron-phonon interaction  $G_{\text{el-ph}}$  to be strong. One may write a Hamiltonian describing the coupling of the localized electron to the phonon field; it has a form very similar to that of Eq. (2.1), with the important difference being that the electron-phonon coupling  $G_{\text{el-ph}}$  is not of order  $\omega_{\text{ph}}$  but is instead given by the geometric mean of an electronic energy and a phonon energy. We estimate  $G_{\text{el-ph}} \sim \sqrt{t\omega_{\text{ph}}}$ , although it is possible that instead of  $t$  one should use an even larger value set by the Coulomb interaction at an interatomic distance. The much larger value of  $G_{\text{el-ph}}$  means that one must go beyond the self-consistent one-boson-exchange approximation employed in this paper. We believe the physics of this model would be that of a small polaron localized to two lattice sites, and suggest that it may explain the observed peak at  $E_J$ . We will present a more detailed study in a subsequent paper.

## ACKNOWLEDGMENT

We thank G. A. Thomas for many helpful discussions of the data and their interpretation.

## APPENDIX A

In this appendix we derive the effective Hamiltonian governing the coupling of a strongly bound carrier to the ordered moment and spin-wave excitations of a two-sublattice Néel antiferromagnet. We assume the impurity potential which binds the carrier is symmetric under the interchange of the two sublattices of the antiferromagnet. In the presence of even a short-range AFM correlation it is convenient to double the unit cell and explicitly introduce sublattice indices  $A, B$ . One is then naturally let to consider four carrier states labeled by the  $z$  component of the spin,  $\sigma = \pm 1$ , and the sublattice index  $\alpha = A, B$ :  $|\alpha, \sigma\rangle$ . Since the carrier hopping matrix element,  $t$ , mixes  $A, B$  sublattice states, one immediately expect to find a “bonding” to “antibonding” energy gap  $\sim O(t)$  separating states even and odd under the  $A \leftrightarrow B$  interchange. The nonvanishing value of the staggered magnetization,

$$\Omega \equiv \langle \bar{\Omega} \rangle = \frac{1}{2N} \left\langle \sum_{i \in A} \bar{S}_i - \sum_{i \in B} \bar{S}_i \right\rangle \neq 0,$$

breaks parity (reflection on bonds) and makes the bonding-antibonding wave functions asymmetric, with charge distribution dependent on the spin. However, the combined operation of the sublattice interchange and time reversal, which flips all spins, not only commutes with the Hamiltonian but also leaves the Néel ground state invariant. This leads to Kramer’s degeneracy: the four states under consideration form two doublets, which we denote as  $|\nu, \sigma\rangle$  with  $\nu=1$  referring to the ground (“bonding”) state and  $\nu=2$  to the excited (“antibonding”) state and  $\sigma$  being the eigenvalue of spin along the direction of staggered magnetization,  $\hat{\Omega}$ .

We may explicitly derive the Hamiltonian for the simple model shown in Fig. 2. Here the impurity potential is assumed to be so strong that it localizes the carrier onto one of the two sites surrounded by the dotted line. On the site not occupied by the carrier a spin resides. The defect has four states, which we label by the site on which the spin resides and the direction of the spin, thus we have states  $|b \uparrow\rangle, |b \downarrow\rangle, |a \uparrow\rangle, |a \downarrow\rangle$ . These states are coupled by the hopping matrix element  $t$  and by the Heisenberg interaction between the spin on site  $A$  or  $B$  and the spins on the three nearest neighbors of that site. We treat the magnetic degrees of freedom on the remaining sites in the crystal within the linearized spin-wave approximation,<sup>17</sup> and we neglect the effect of the impurity on the spin-wave spectrum. We treat exactly the part of the Hamiltonian involving the hopping and the coupling to the Néel order parameter. We retain the leading-order spin-wave operators as a perturbation. Neglecting at first the spin-wave operators, we diagonalize the remaining terms, obtaining the four states  $|b \uparrow\rangle, |b \downarrow\rangle, |a \uparrow\rangle, |a \downarrow\rangle$  which are related to the original states via

$$\begin{aligned} |b, \uparrow\rangle &= \cos\theta |A, \uparrow\rangle + \sin\theta |B, \uparrow\rangle, \\ |b, \downarrow\rangle &= -\sin\theta |A, \downarrow\rangle - \cos\theta |B, \downarrow\rangle, \\ |a, \uparrow\rangle &= \sin\theta |A, \uparrow\rangle - \cos\theta |B, \uparrow\rangle, \\ |a, \downarrow\rangle &= -\cos\theta |A, \downarrow\rangle + \sin\theta |B, \downarrow\rangle, \end{aligned} \quad (\text{A1})$$

with bonding-antibonding splitting  $\Delta$  and mixing angle  $\theta$  given by

$$\Delta = 2\sqrt{t^2 + (3J\Omega)^2}, \quad (\text{A2a})$$

$$\cos\theta = \left[ \frac{1}{2} + \frac{3J\Omega}{\Delta} \right]^{1/2}. \quad (\text{A2b})$$

If we now transform into the new basis, the coupling between the impurity spin and the fluctuating part of the magnetic degrees of freedom of the crystal, takes the form of the Hamiltonian (2.1) with

$$g_1 = \frac{1}{2}J \sin 2\theta, \quad (\text{A3a})$$

$$g_2 = \frac{1}{2}J \cos 2\theta, \quad (\text{A3b})$$

$$g_3 = \frac{1}{2}J, \quad (\text{A3c})$$

and

$$\begin{aligned} M_k &= (\text{Re}\lambda_k)(\cosh Q_k - \sinh Q_k) \\ &\quad + i(\text{Im}\lambda_k)(\cosh Q_k + \sinh Q_k), \end{aligned} \quad (\text{A4a})$$

$$\begin{aligned} N_k &= \text{Re}\lambda_k(\cosh Q_k + \sinh Q_k) \\ &\quad + i(\text{Im}\lambda_k)(\cosh Q_k - \sinh Q_k) \end{aligned} \quad (\text{A4b})$$

with (the sites  $i_1$  are the three nearest neighbors of impurity site 1)

$$\lambda_k = \sum_{i_1} e^{ik \cdot i_1} \quad (\text{A5})$$

and  $\cosh Q_k$  is related to the spin-wave energy  $\omega_k$  via

$$\cosh 2Q_k = 1/\omega_k. \quad (\text{A6})$$

We emphasize that while the above construction becomes exact for the carrier localized on two sites and coupled to the background by spin exchange, it should be thought of in a more general context, with states  $|b(a), \sigma\rangle$  representing approximate Brinkman-Rice “string” states<sup>18</sup> which allow for carrier excursions away from a given site, and lead to renormalization of the hopping (and the current) matrix elements. Also, in general the dipole moment will be distributed among a number of excited states, which should then be included. A practical computational scheme consists of picking a small cluster containing the carrier and the localizing potential. One can then diagonalize the cluster Hamiltonian in the presence of the frozen external staggered field. Evaluating the matrix elements of the charge current and spin exchange for the cluster eigenstates, one will arrive at the effective Hamiltonian describing the coupling of the cluster states with the environment.

## APPENDIX B

In this appendix we give details of the canonical transformation leading from (2.1) to (3.4) and (3.5a). We write the Hamiltonian,  $H$ , of Eq. (2.1) in the form

$$H = H_0 + H_m, \quad (\text{B1})$$

where  $H_0$  includes the terms proportional to  $\Delta$  and  $g_1$

which do not mix the  $b$  and  $a$  states and  $H_m$  includes the  $g_{2,3}$  terms which do mix the states. We seek a canonical transformation,  $iS$ , such that

$$H' = e^{iS} H e^{-iS} \quad (\text{B2})$$

does not mix  $A$  and  $B$  states. We construct this transformation perturbatively in  $g_{2,3}/\Delta$ . Thus, we require

$$[iS, H_0] = -H_m. \quad (\text{B3})$$

We write

$$iS = - \sum_k (c_{a\uparrow b\downarrow}^\dagger + c_{b\uparrow a\downarrow}^\dagger) U_k (\alpha_k^\dagger + \beta_k) \\ + (c_{a\uparrow b\downarrow}^\dagger - c_{b\uparrow a\downarrow}^\dagger) V_k (\alpha_k^\dagger - \beta_k) \\ - \text{H.c.} \quad (\text{B4})$$

After substituting (B4) and (B3) we find

$$U_k = \frac{\Delta g_2 M_k + \omega_k g_3 N_k}{\Delta^2 - \omega_k^2}, \quad (\text{B5a})$$

$$V_k = \frac{\omega_k g_2 M_k + \Delta g_3 M_k}{\Delta^2 - \omega_k^2}. \quad (\text{B5b})$$

Once  $U_k$  and  $V_k$  are determined we may compute the transformation of the vector potential term by evaluating  $e^{iS} H_A e^{-iS}$  with  $H_A$  given by Eq. (2.2); the result is Eq. (3.5a).

<sup>1</sup>P. W. Anderson, *Science* **235**, 1196 (1987).

<sup>2</sup>N. W. Preyer, R. J. Birgeneau, C. Y. Chen, D. R. Gabbe, H. P. Jenssen, M. A. Kastner, P. J. Picone, and T. Thio, *Phys. Rev. B* **39**, 11 563 (1989).

<sup>3</sup>S. L. Cooper, G. A. Thomas, A. J. Millis, P. E. Sulewski, J. Orenstein, D. Rapkine, S.-W. Cheong, and P. L. Trevor, *Phys. Rev. B* **42**, 10 785 (1990).

<sup>4</sup>N. W. Preyer, R. J. Birgeneau, C. Y. Chen, D. R. Gabbe, H. P. Jenssen, M. A. Kastner, P. J. Picone, and T. Thio, *Phys. Rev. B* **39**, 11 563 (1989).

<sup>5</sup>K. Rabe and R. Bhatt, *J. Appl. Phys.* **69**, 4508 (1991).

<sup>6</sup>G. A. Thomas, D. M. Rapkine, S. L. Cooper, S.-W. Cheong, A. S. Cooper, L. F. Schneemeyer and J. V. Waszczak, *Phys. Rev. B* **45**, 2474 (1992).

<sup>7</sup>M. S. Hybertsen, E. B. Stechel, M. Schluter, and D. R. Jennison, *Phys. Rev. B* **41**, 11 068 (1990).

<sup>8</sup>E. B. Stechel and D. R. Jennison, *Phys. Rev. B* **38**, 4632 (1988); **38**, 8873 (1988).

<sup>9</sup>G. A. Thomas (private communication). See also Refs. 4 and 6.

<sup>10</sup>It could be that because the  $\text{CuO}_2$  lattice is highly polarizable it will distort itself on long length scales in response to the electrostatic potential of an unscreened dopant ion. However, if the carrier is tightly bound to the dopant ion, the resulting entity is neutral on long length scales and so causes no lattice distortion. Thus, one imagines two relatively low-energy states, one with a bound carrier and no lattice distortion and one with no bound carrier but a lattice distortion. The energy difference between these two states would be important for a thermally activated process such as hopping conductivity, but would not show up either in a theoretical calculation, which did not include the possibility of a long-range lattice distortion, or in an optical absorption experiment in which

the impurity was ionized while the lattice did not have time to relax.

<sup>11</sup>Within the approximation used here the  $\delta$ -function peak exists for all values of the interaction strength,  $\lambda$ . Further, we believe that the peak must exist for sufficiently small  $\lambda$  in spatial dimension  $d > 1$  because symmetry considerations dictate that the only low-energy excitations in which the impurity spin is flipped involve fluctuations of the magnetization (for which the density of states vanishes as  $\omega_k \rightarrow 0$ ) and not the staggered magnetization (for which the density of states diverges as  $\omega_k \rightarrow 0$ ). It is an interesting open question whether, in  $d > 1$  for  $\lambda$  sufficiently large, the coefficient of the  $\delta$ -function vanishes. This would correspond to an analog of the Kondo effect, where the character of a local moment is fundamentally altered by its coupling to a bath of excitations. This possibility is presently under investigation. In the balance of this paper we assume that at  $T=0$  the spectral function includes a term proportional to  $\delta(\omega)$ .

<sup>12</sup>S. Hayden, G. Aeppli, R. Osborn, A. D. Taylor, T. G. Perring, S.-W. Cheong, and Z. Fisk (unpublished).

<sup>13</sup>W. F. Brinkman and T. M. Rice, *Phys. Rev. B* **2**, 1324 (1970); L. N. Bulaevskii, E. L. Nagaev, and D. I. Khomskii, *Zh. Eksp. Teor. Fiz.* **54**, 1562 (1968) [*Sov. Phys. JETP* **27**, 836 (1968)].

<sup>14</sup>S. Trugman, *Phys. Rev. B* **37**, 1597 (1988); V. Elser, D. A. Huse, B. I. Shraiman, and E. D. Siggia, *ibid.* **41**, 6715 (1990).

<sup>15</sup>C. Kane, P. Lee, and N. Read, *Phys. Rev. B* **39**, 6880 (1989).

<sup>16</sup>T. M. Rice and F. C. Zhang, *Phys. Rev. B* **39**, 815 (1989).

<sup>17</sup>Our notation follows C. Kittel, *Quantum Theory of Solids* (Wiley, New York, 1963).

<sup>18</sup>B. I. Shraiman and E. D. Siggia, *Phys. Rev. B* **42**, 2485 (1990).